Technical Report

TR-09-33

Bentonite erosion

Laboratory studies

Mats Jansson, Nuclear Chemistry, KTH

November 2009

Svensk Kärnbränslehantering AB
Swedish Nuclear Fuel
and Waste Management Co

Box 250, SE-101 24 Stockholm
Phone +46 8 459 84 00

Bentonite erosion

Laboratory studies

Mats Jansson, Nuclear Chemistry, KTH

November 2009

Summary

This report covers the laboratory studies that have been performed at Nuclear Chemistry, KTH in the project "Bentonite Erosion". Many of the experiments in this report were performed to support the work of the modelling group and were often relatively simple.

One of the experiment series was performed to see the impact of gravity and concentration of mono- and di-valent cations. A clay suspension was prepared in a test tube. A net was placed in contact with the suspension, the test tube was filled with solutions of different concentrations and the system was left overnight to settle. The tube was then turned upside down and the behaviour was visually observed. Either the clay suspension fell through the net or stayed on top. By using this method surprisingly sharp determinations of the Critical Coagulation (Flocculation) Concentration (CCC/CFC) could be made. The CCC/CFC of Ca^{2+} was for sodium montmorillonite determined to be between 1 and 2 mM.

An artificial fracture was manufactured in order to simulate the real case scenario. The set-up was two Plexiglas slabs separated by 1 mm thick spacers with a bentonite container at one side of the fracture. Water was pumped with a very low flow rate perpendicular to the bentonite container and the water exiting the fracture was sampled and analyzed for colloid content. The bentonite used was treated in different ways. In the first experiment a relatively montmorillonite rich clay was used while in the second bentonite where only the readily soluble minerals had been removed was used.

Since Plexiglas was used it was possible to visually observe the bentonite dispersing into the fracture. After the compacted bentonite (1,000 kg/m^3) had been water saturated the clay had expanded some 12 mm out into the fracture. As the experiment progressed the clay expanded more out into the fracture and seemed to fractionate in two different phases with less material in the outmost phase. A dark rim which was later analyzed to contain mostly feldspar developed at the border between the two phases.

After 45 weeks the clay had expanded some 20 cm into the fracture. The colloid content in the outlet solution was however stable and less than 200 mg/l. The size of the colloids was however much smaller than that obtained when MX-80 is dispersed in water. The development of the clay profile into the fracture and the colloid content in the outlet solutions were the same in both experiments.

In one of the fracture experiments the fracture was tilted, inclining some 2–3 degrees with the higher end at the water outlet. A relatively thick gel accumulated at the inlet side of the fracture, *i.e.* the clay sedimented towards the water flow, clearly showing that gravity plays a big role in this system.

Sammanfattning

Den här rapporten avhandlar de försök som gjorts på avdelningen Kärnkemi, KTH, i projektet ”Bentonite Erosion”. Mycket av arbetet skedde i nära samarbete med projektets modelleringsgrupp och många försök var relativt enkla och gjordes för att testa olika parametrars inverkan på systemet bentonit-vatten.

I ett av försöken undersöktes påverkan av gravitation och koncentration av mono- och di-valenta katjoner. En lersuspension framställdes i ett provrör och ett nät som hölls på plats mha en o-ring placerades direkt ovanför suspensionen. Provröret fylldes med lösningar med olika koncentrationer av katjoner och lämnades därefter. Dagen efter vändes provröret upp-och-ner. Antingen föll leran genom nätet inom 5–15 minuter eller annars stannade den kvar under längre tider (några prover observerades upp till två månader). Denna metod gav överraskande tydliga svar. Den s.k. kritiska koaguleringskoncentrationen (”Critical Coagulation (Flocculation) Concentration”, CCC/CFC) kunde för kalciumjoner bestämmas vara mellan 1 och 2 mM för ren natrium-montmorillonit.

En försöksuppställning med en konstgjord spricka byggdes för att simulera det verkliga scenariot. Uppställningen bestod av två plexiglasskivor som hölls skiljda av ett antal 1 mm tjocka plastbrickor. På ena sidan av sprickan fanns en bentonitbehållare. Vatten pumpades vinkelrätt mot bentonitbehållaren genom sprickan med en mycket låg flödeshastighet och vatten från utloppet analyserade med avseende på kolloidkoncentration. Bentoniten som användes var förbehandlad på olika sätt. I det första försöket användes en montmorillonitrik lera medan en lera där bara lättlösliga mineraler hade tagits bort användes i det andra försöket.

Eftersom plexiglas användes kunde man visuellt observera hur bentoniten trängde ut i sprickan. Efter att den kompakterade bentoniten (1 000 kg/m^3) hade vattenmättats, vilket gjordes via en kanal på bentonitbehållarens baksida, hade leran trängt ut ca 12 mm i sprickan. Vatten började sedan pumpas genom sprickan och leran expanderade ut alltmer. Man kunde observera att leran tycktes fraktionera i två olika faser med en fas som avgjort hade lägre lerhalt längs ut. En svart rand, som senare analyserades till att bestå av mestadels fältspat, byggdes upp mellan de två faserna.

Efter 45 veckor hade leran expanderat ca 20 cm ut i sprickan. Kolloidhalterna i vattnet som lämnade sprickan var dock konstanta genom hela försöket och mindre än 200 mg/l. Storleken på kolloiderna var dock avsevärt mindre än storleken som erhålls när man dispergerar MX-80 bentonit i vatten. Man kunde inte se någon skillnad mellan de två försöken avseende hur profilen byggdes upp i sprickan och hur mycket kolloider som kom ut ur sprickan.

I det andra försöket lutades sprickan 2–3 grader med den högre änden vid vattnets utlopp. En relativt tjock gel av lera ackumulerades vid sprickans inlopp, dvs. leran sedimenterade mot vattenflödet, vilket klart visar att gravitationen spelar en relativt stor roll i det här systemet.

Contents

1 Introduction and Background

Bentonite clay has been proposed as buffer material in the KBS-3 concept of storing spent nuclear fuel. Since the clay is plastic it will protect the canisters containing the spent fuel from movements in the rock. Furthermore, the clay will expand when taking up water, become very compact and hence limit the transport of solutes to and from the canister to only diffusion.

The chemical stability of the bentonite barrier is of vital importance. If much material would be lost the barrier will lose its functions. There are scenarios where during an ice age fresh melt water may penetrate down to repository depths with relatively high flow rates /Liu and Neretnieks 2006/. Under such conditions bentonite colloids will be more stable and there is a possibility that the bentonite buffer would start to disperse and bentonite colloids be carried away by the passing water.

The project "Bentonite Erosion" has during the past years been looking in more detail on the processes that may occur and under what circumstances. This report covers the laboratory work that has been performed at Nuclear Chemistry, KTH, mainly to support the work of the modelling group.

2 Aims and Scope

The laboratory studies at Nuclear Chemistry have been performed in a close co-operation with the modelling group. Many of the experiments have been performed to see how the system in general responds to changes in different parameters. This was often involved the use of relatively simple experiments.

The following problems were addressed:

- What is the impact of gravity? This was addressed both in the test tube experiments and in the artificial fracture.
- How does bentonite (montmorillonite) behave in different salinities? Is it only the ionic strength that is important or does the valence of the ions play a role? An attempt to quantify the concentrations of different cations that are needed to keep bentonite from dispersing was made.
- How far will unconfined sodium montmorillonite swell and how will the clay concentration profile look?

A larger experiment was performed where an artificial fracture was manufactured to simulate the real case. In this experiment the primary aim was to see if bentonite colloids would be released and carried by the seeping water and if so, in what concentrations. Another objective was to visually observe the progress of the dispersion process.

3 Purification of Montmorillonite

Since montmorillonite is the key mineral in bentonite and also the component that is suspected to disperse and eventually be removed from the buffer by the flowing groundwater, in many of the investigations pure montmorillonite (altered to contain only one kind of exchangeable cation) was used.

To obtain pure sodium montmorillonite a relatively tedious process described by /Sposito et al. 1981/ was employed. The method described comprises the following steps:

1. Disperse 50 g bentonite in 0.8 dm^3 of 0.001 M HNO_3, 1 M $NaNO_3$ solution.
2. Shake 20 min, centrifuge 10 min, 4,000 rpm, remove supernatant.
3. Measure pH of supernatant.
4. Repeat step 1–3 until pH ≈ 3. This requires about 10 cycles.
5. Disperse in 1.2 dm^3 0.1 M $NaNO_3$.
6. Shake 20 min, centrifuge 10 min, 4,000 rpm, remove supernatant.
7. Measure pH of supernatant.
8. Repeat step 5–7 until pH = 5.1–5.3. This requires 10–15 cycles. The last two cycles should be performed with 0.01 M $NaNO_3$ solution under Argon atmosphere.

In order to remove heavier accessory minerals the clay fraction obtained in step 2 was separated into two fractions during the first three cycles. The heavier blackish fraction was removed and the lighter montmorillonite rich fraction was used for further treatment.

In later experiments purified sodium and calcium montmorillonites obtained from Clay Technology were used. Clay Technology used a more efficient process /Karnland et al. 2006/:

1. Disperse 10 g bentonite in 1.0 dm^3 of de-ionized water.
2. Add NaCl to obtain a 1 M solution. Let the material settle. Remove supernatant.
3. Repeat step 1 and 2 three times.
4. Add de-ionized water. Centrifuge.
5. Repeat step 4 until dispersion starts.
6. Transfer slurry except the sedimented coarsest material to dialysis membrane.
7. Change the water outside the membrane daily until the conductivity stabilizes below 10 μS/cm.
8. Disperse material in de-ionized water and remove d >2 μm fraction by sedimentation.
9. Repeat step 1–8.
10. Dry the material at 60°C and grind to an aggregate size similar to that of MX-80.

For both methods the purified material obtained was analyzed by ICP-MS in order to ensure that the material was fully cation exchanged.

4 Analyses of Colloids

The colloid concentrations were measured using two different methods; Photon Correlation Spectroscopy (PCS) and Single Particle Counter (SPC). The two methods have different advantages and drawbacks. Analyzing samples on the PCS is much more time efficient while the SPC can detect colloids at lower concentrations.

4.1 Photon Correlation Spectroscopy

The PCS method is developed mainly to study the size distribution of particles in a sample. The sample is kept at constant temperature and irradiated by a laser beam and the scattering of the light is detected. Since the particles move by Brownian motion, the scattering will differ with time. Larger particles will move with a lower rate than smaller particles. If the diffusivity of the particles and the viscosity of the solution are known, the size of the particles can be determined using Stokes-Einstein's relation (which assumes spherical particles).

The PCS method also gives a measure of the number of particles that has given rise to the scattering (intensity). If the particles have a homogeneous size distribution the intensity is a measure of the particle concentration.

According to /Plaschke et al. 2001/ montmorillonite colloids are not spherical but disc-shaped, hence the PCS overestimates the larger sized particles (>200 nm). Furthermore, the method is relatively insensitive for small particles in presence of larger particles since the larger particles shield the smaller /Plaschke et al. 2001/.

4.2 Single Particle Counter

To be able to measure very low colloid concentrations either a Single Particle Counter (SPC) or Laser Induced Breakdown Detection (LIBD) techniques need to be employed. The handling of a LIBD is easier than that of a SPC, but a LIBD instrument costs ten times more than a SPC. At Nuclear Chemistry a SPC is available.

The principle of SPC is that a continuous flow (about 100 ml/min) of distilled water passes through a detector which consists of a laser and a photocell. Each particle passing through the beam causes a small scattering of the light. The scattering is greater for larger particles and the SPC divides the particles in four size ranges; 0–50, 50–100, 100–200 and >200 nm. When analyzing a sample with the SPC, the sample is sucked into an automated injector and is then injected into the continuous flow with a flow rate of typically 1 ml/min.

The method is rather time consuming since very small disturbances often cause large errors and sometimes samples have to be analyzed several times in order to get a reliable result. If a sample with relatively high colloid content is analyzed it takes up to an hour for the instrument to stabilize. If the outlet of the continuous flow is raised a decimeter it causes a small change in pressure, which in turn affects the flow and gives a disturbance in the signal from the instrument. A gas-bubble in the flow path disturbs the signal significantly and has to be removed, which in turn requires alteration of the flow and further time to stabilize the instrument. All in all, the SPC is a very sensitive instrument in terms of low detection limits but also in terms of handling.

Another thing that adds to the uncertainty of the results is the water purification unit at Nuclear Chemistry, which has during the years degraded. An ion-exchanger releases small particles (<100 nm), which affects results in the two lower channels of the SPC. This was not detected before the SPC was purchased, since the PCS is not sufficiently sensitive.

5 Test Tube Studies

5.1 Background

Colloid stability is very much affected by the salinity of the colloidal solution. At a certain cation concentration colloids agglomerate. There is some confusion in the literature regarding how this concentration is defined and even what it should be called. The critical concentration is sometimes called the Critical Coagulation Concentration (CCC) while other claim that coagulation is an irreversible process and the correct name should be Critical Flocculation Concentration (CFC).

Some claim that the CCC/CFC is the concentration where the attractive and repulsive forces acting on the colloids are equal /García-García et al. 2007/, according to the DLVO-theory /Derjaguin and Landau, 1941, Verwey and Overbeek 1948/. Others defines the concentration empirically by visual inspection or by turbidity measurements /Goldberg et al. 1991/ after a certain time. Another frequently used method is to study the rheological behaviour /Lagaly and Ziesmer 2003/ while yet other groups defines a kind of stability coefficient and thereby avoid setting a specific value. Hence the CCC/CFC-values vary in the literature.

For montmorillonite colloids (as for most negatively charged colloids) the concentration of divalent cations is more important than the concentration of monovalent cations. The CCC/CFC is about one to two orders of magnitude less for divalent cations compared to monovalent cations.

5.2 Solubility of $CaCO_3$

Bentonite usually contains some percent (s) calcium containing minerals; mainly calcite and gypsum. Gypsum has a solubility of about 12 mM in pure water and will probably dissolve and leave the system at an early stage. This is discussed in more detail by /Neretnieks et al. 2009/ Calcite is however more interesting. Since the solubility of calcite at buffer pH is relatively close to reported CCC/CFC concentrations for Ca^{2+}, it is of keen interest to the Bentonite Erosion project to further investigate what calcium concentrations which are critical for bentonite.

The following equilibira governs the solubility of $CaCO_3$ in water /Stumm and Morgan 1996/:

$$CaCO_3(s) \rightleftharpoons Ca^{2+}(aq) + CO_3^{2-}(aq) \qquad K_{s0} = 10^{-8.3}\ M2 \tag{5-1}$$

$$CO_3^{2-}(aq) + H+(aq) \rightleftharpoons HCO_3^{-}(aq) \qquad K_2 = 10^{10.2}\ M \tag{5-2}$$

$$HCO_3^{-}(aq) + H^{+} \rightleftharpoons H_2O + CO_2(aq) \qquad K_1 = 10^{6.3} \tag{5-3}$$

$$CO_2(aq) \rightleftharpoons CO_2(g) \qquad K_H = 10^{1.5} \tag{5-4}$$

Summarizing reactions (5.1) to (5.4) gives the following equilibrium:

$$CaCO_3(s) + 2\ H^{+} \rightleftharpoons Ca^{2+}(aq) + CO_2(g) + H_2O \qquad K_{s0}(K1K2KH)^{-1} = 10^{9.7} \tag{5-5}$$

or

$$\left[Ca^{2+}\right] = \frac{10^{7.9}}{P_{CO_2}}\left[H^{+}\right]^2 \tag{5-6}$$

In addition to the four equilibria, the electro-neutrality (charge balance) is needed to compute the composition of species:

$$2\ [Ca^{2+}] + [H^{+}] = [HCO_3^{-}] + 2\ [CO_3^{2-}] + [OH^{-}] \tag{5-7}$$

or approximately

$2\,[Ca^{2+}] = [HCO_3^-]$ 5-8

The $CaCO_3$-system was simulated using the code Medusa Chemical Diagrams /Ignasi Puigdomenech 2009/. In Figure 5-1 the logarithm of the maximum Ca^{2+} concentration is plotted at different pH and in equilibrium with different partial CO_2 pressures. In Appendix I all equilibria upon which the diagram is based are listed.

At normal repository conditions calcite will not dissolve. However, if during an ice age, glacial water penetrates to repository depths the conditions will change. /Arcos et al. 2006/ have modeled the geochemical evolution around a KBS-3 type repository under various conditions.

5.3 Performance

To get a rough estimate whether a bentonite will disperse or not in a specific solution, simple tests were performed. The experimental set-up consisted of a sampling tube equipped with a net which rests on an o-ring, see Figure 5-2. With this set-up the influence of gravity is studied specifically.

0.2 g clay was dispersed (by shaking and using ultra sound) into 10 ml distilled water at the bottom of a sampling tube. A fine net with an o-ring as support was placed immediately above (in contact with) the clay suspension. The rest of the tube (roughly 35 ml) was then filled with a solution with a specific concentration before the cap was placed at the top of the tube.

After 1 day the sampling tube was turned upside-down. The response was easy to observe visually within 5 minutes. Either the clay dispersed and started to fall through the net or else it stayed above the net. Some tubes where the clay stayed above the net were left for 1 month (for instance untreated MX-80 in distilled water) without anything happening. A number of differently treated clays and water compositions were examined using this method. The results confirmed that the Ca^{2+} concentration is a crucial parameter.

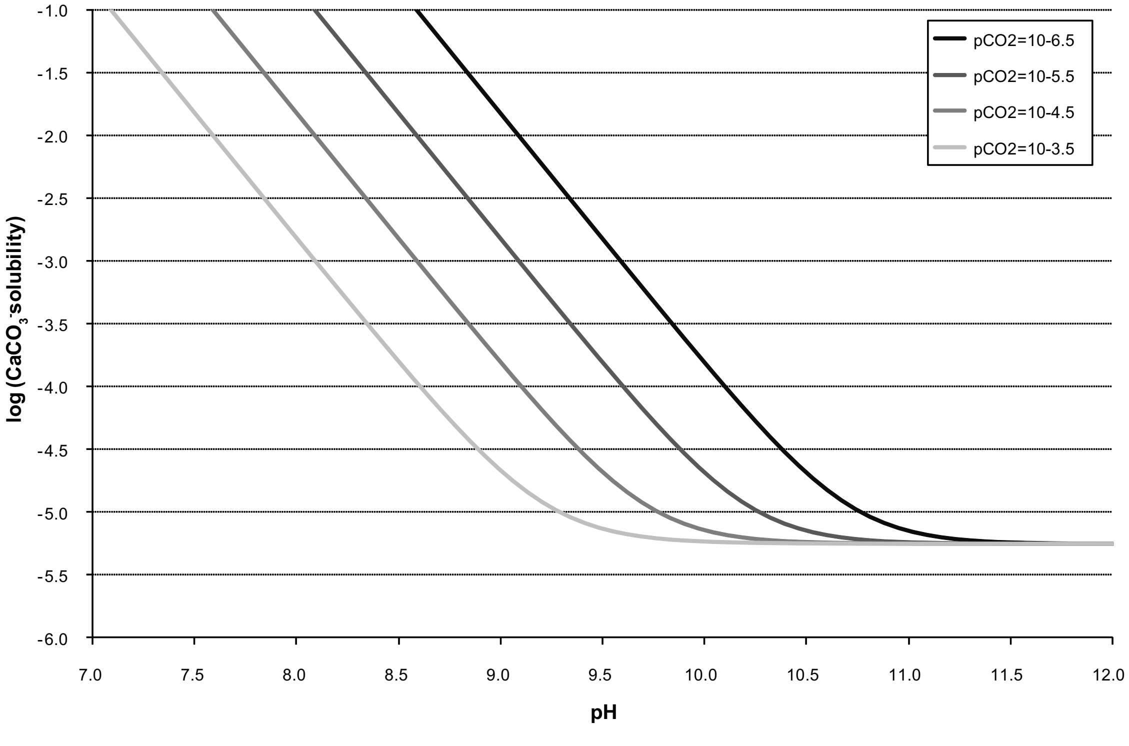

Figure 5-1. *The solubility of $CaCO_3$ as a function of pH. The data is modeled with Medusa Chemical Diagrams, see also Appendix I.*

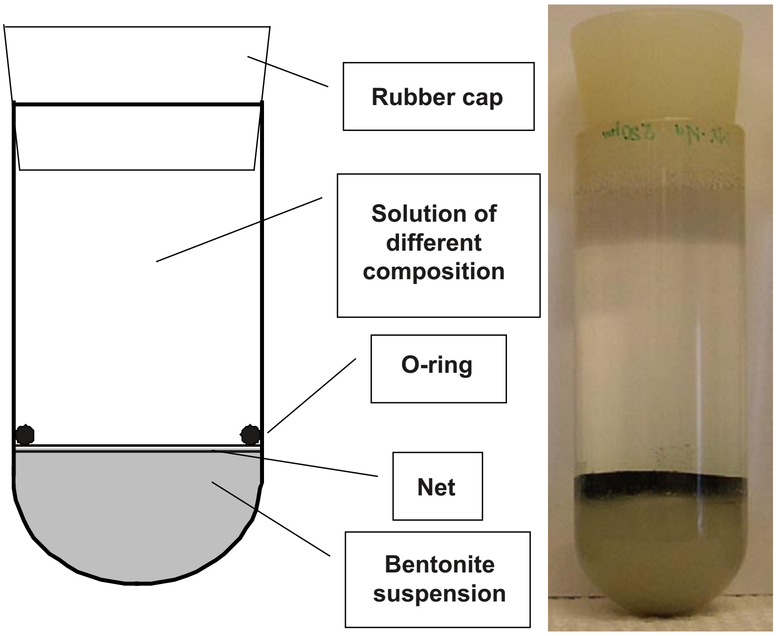

Figure 5-2. *Experimental set-up for the test tube studies.*

5.4 Results and Discussion

The determination of the CCC/CFC concentration for calcium gave a surprisingly easily definable value when purified sodium montmorillonite was examined. When 3 mM Ca-concentration solution was added (giving a total Ca^{2+} concentration of 2.33 mM) the clay definitely stayed above the net, while when 1 mM Ca-solution was added (giving a total Ca^{2+} concentration of 0.78 mM) all of the clay fell through, see Figure 5-3.

Bentonite clay buffers a system to a pH of about 8.2. From Figure 5-1 we find that at pH 8.2 the maximum Ca^{2+} concentration is about 0.6 mM if the system is in equilibrium with atmospheric CO_2. The conclusion is thus that the Ca^{2+}-concentration from dissolving calcite is not sufficient to stop Na-montmorillonite from dispersing at atmospheric CO_2 pressures.

However, when the partial pressure of CO_2 decrease, the solubility of $CaCO_3$ increase. In a pure $CaCO_3$-water system a partial pressure of CO_2 of about 80 μbar corresponds to the obtained Ca^{2+} concentration in this study (2.33 mM).

A mass balance on the experiment gives the following: Purified sodium montmorillonite has a cation exchange capacity of about 0.85 milli-equivalents per gram /Muurinen and Lehikoinen 1997/. 0.2 gram Na-montmorillonite has thus roughly 0.17 mmol sites. Since the calcium ion is divalent each ion will occupy two sites and the number of available sites in 0.2 gram Na-montmorillonite is for calcium 8.5×10^{-5} mol. Approximately 35 ml solution with a Ca^{2+} concentration of 2 mM was added, which corresponds to 7.0×10^{-5} mol. The number of available sites was thus in the same order of magnitude as the number of Ca^{2+} ions.

Another test was hence performed using ten times less bentonite than in the tests described above. Due to the lower clay content, the gel formed was looser. However, when turning the test tubes upside-down, similar behaviour was observed as when using more clay, indicating that the calcium concentration is the crucial parameter rather than the amount of Ca^{2+} ions available, see Figure 5-4.

As can be seen, in the 3–5 mM tubes there is clearly gels that stays above the net, while at 1 mM Ca^{2+} concentration all montmorillonite is more or less dispersed in the whole tube. One can observe slightly higher clay concentrations at the top of the test tube in the 1 mM case, but this was levelled out when the tube was left for a couple of days.

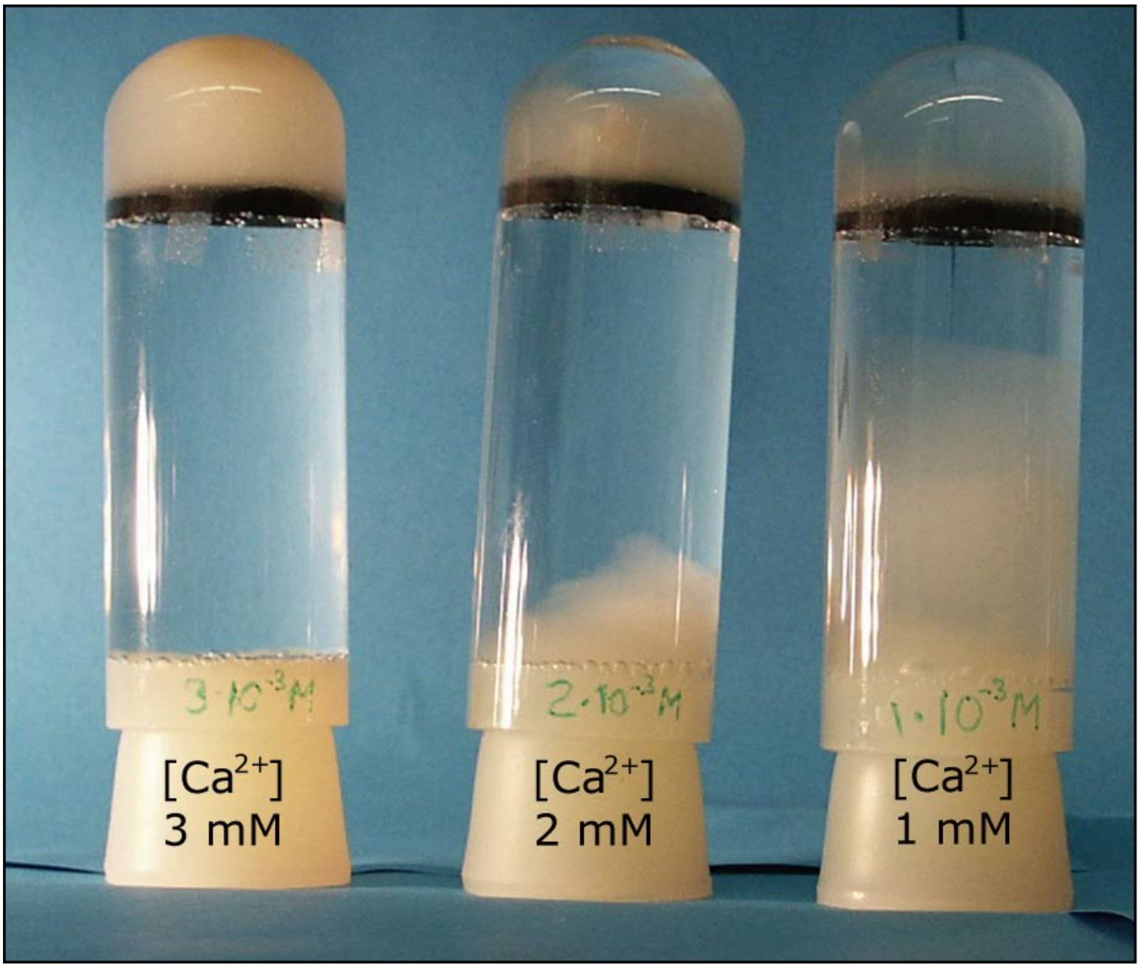

Figure 5-3. *Determination of lowest Calcium concentration needed to keep pure sodium montmorillonite from dispersing. Note that the concentrations are the values for the added solution to the 10 ml clay suspension.*

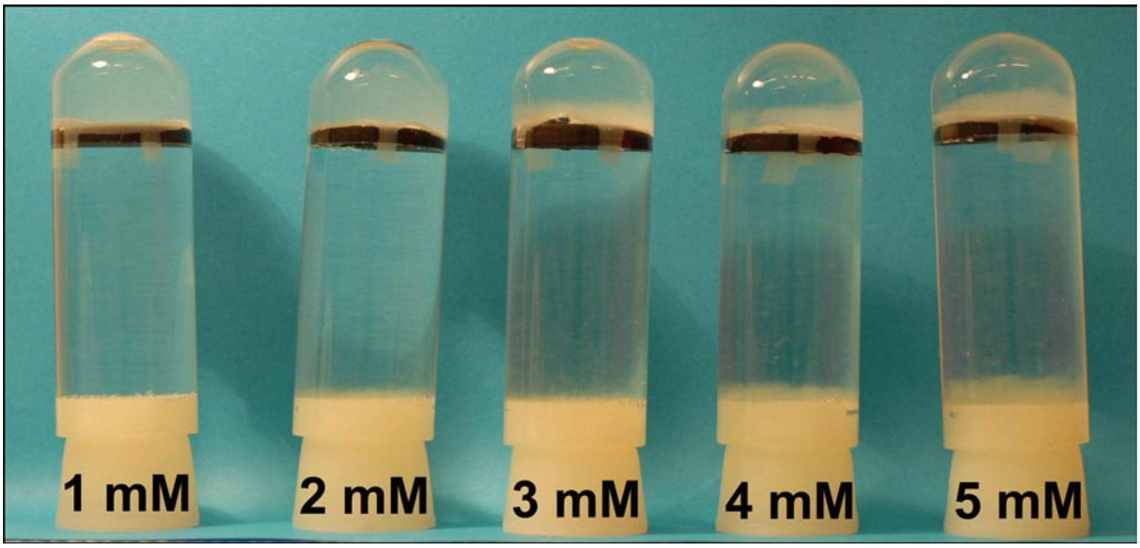

Figure 5-4. *Determination of lowest Calcium concentration needed to keep sodium montmorillonite from dispersing using ten times lower clay content than in the previous test.*

Furthermore, one can observe a gel at the bottom of test tubes containing 4 and 5 mM Ca^{2+}. This is due to the preparation of the test tubes. Since trapped air disturbs the experiment, the net with the o-ring is pushed slightly below the surface of the gel solution when the sample is prepared. This causes some gel to be on the wrong side of the net when the tubes are top-filled and turned up-side down.

A number of studies were performed using the same experimental set-up as described above. The results were not as sharp as the one for calcium and sodium montmorillonite. The main findings were:

- The size of the net is not important. Three different hole sizes were studied; 250, 45 and 10 µm. The only observed difference was that it took twice as long time to fall through the 45 µm net compared to the 250 µm net; 10 instead of 5 minutes.
- Non-treated MX-80 bentonite did not fall through the net at any calcium or sodium concentration. A set-up with MX-80 and distilled water was observed for three months.
- MX-80 bentonite that had been washed twice with distilled water (40 ml water/g clay) in order to remove readily soluble minerals, especially gypsum, behaved similarly as sodium montmorillonite. The obtained CCC/CFC value was slightly higher (3 mM), though.
- One test was performed to see how the system behaved when the suspension was left up-side down to stabilize for longer periods of time (1 month). The clay settled, though, and was not a suspension anymore. In some of the test tubes there was an air bubble (originating from when the cap was put in place) over the settled clay and the clay got stuck at the very top of the tube. In other cases the clay stuck to the very top of the test tube when the tube was turned upside down and fell after some time down on the net in relatively large agglomerates. The impact when falling on the net caused some of the clay to fall through. All in all, the results were inconclusive.
- It was not possible to perform conclusive studies on purified calcium montmorillonite, since such clay sticks together more strongly. Large agglomerates fell through the net and some agglomerates stayed on the net at almost any concentration of the solution used. Since the calcium clays stuck together in large agglomerates gravity probably plays a bigger role than in the sodium case.
- The CCC/CFC value for sodium montmorillonite in sodium solution was not as "sharp" as that for the calcium solution. Leaving the samples for 30 minutes allowed a value of 0.1 M to be determined. The clay suspension over the net was not stable over longer periods, however, but dispersed slowly. After three months most of the clay had fallen through the net. That was not the case for calcium where the clay stayed on the net for the whole time the experiment was performed (3 months).

6 Montmorillonite Swelling

6.1 Background

When dry montmorillonite comes in contact with water the exchangeable cations will start to hydrate and the clay sheets will be pushed apart; the clay will start to swell. This is often referred to as crystalline swelling.

Since the cation concentration in the space between the sheets is higher than outside, the chemical potential in the space between the sheets is lower than that on the outside. To compensate for the difference in chemical potential water will be transported to the layers between the sheets. Transport of cations from the space between the sheets is not possible since the system has be electrically neutral. So, even after the exchangeable cations are fully hydrated the clay will continue to take up water. This so called osmotic swelling will theoretically continue indefinitely /Kryut 1952/.

6.2 Performance

To study the swelling and dispersion of sodium montmorillonite 0.2 grams sodium montmorillonite was placed at the bottom of a 45 ml bottle. Distilled water was gently pumped into the bottle in order to not physically disturb the clay (filling the bottle took 2 hours). The height of the visible clay in the bottle was measured visually from photos, see Figure 6-1, and the average density of the clay suspension was calculated, Figure 6-2.

Figure 6-1. Swelling of sodium montmorillonite. The difference in water volume is due to sampling for measuring colloid concentrations. At intervals the water was replenished.

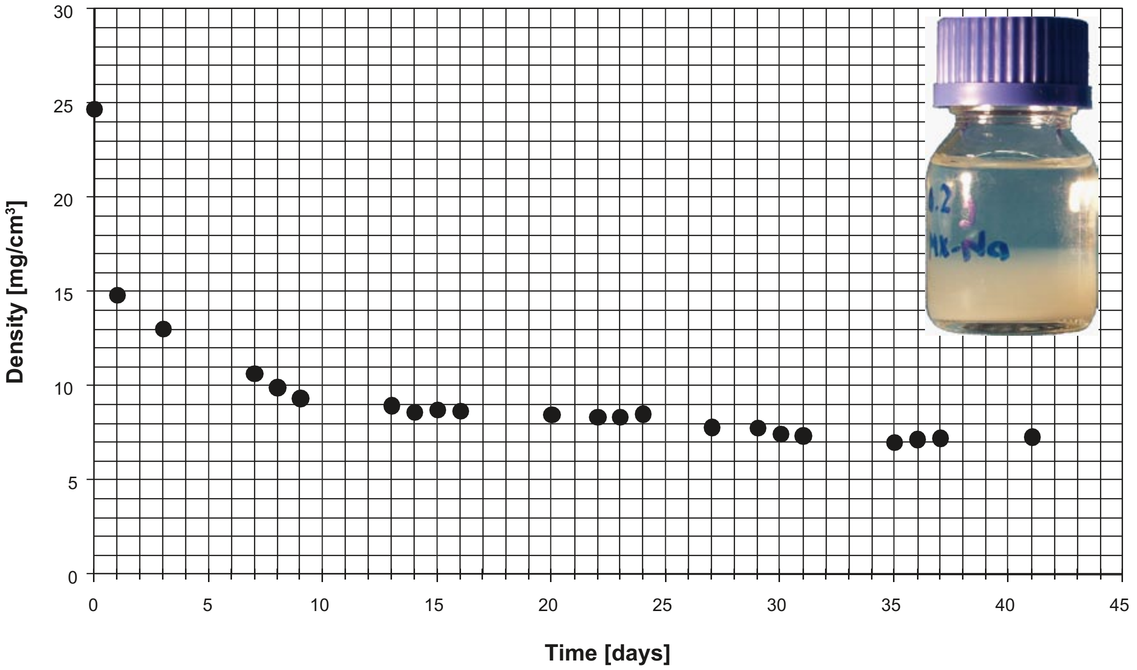

Figure 6-2. *Average density of the swelling sodium montmorillonite. There is a concentration gradient through the clay and the values are an average.*

Throughout the whole period of time of the experiment samples were taken from the very top of the bottle and analyzed using Photon Correlation Spectroscopy (PCS) for colloid concentration and size distribution.

6.3 Results and Discussion

The results from the sampling at the top of the bottles are displayed in Figure 6-3. As can be seen, the effective diameter of bentonite colloids seems to stabilize around 150 nm and the concentration does not exceed 100 ppm. Since 2 ml are needed for the PCS-measurements, the solution in the bottle had to be replenished at intervals (after 8 and 23 days), which is the reason for the low values at these times.

After 41 days the water was slowly pumped out from the top of the bottle and collected in 2.5 ml fractions. Each fraction was analyzed for colloids using PCS. The results are shown in Figure 6-4.

There is a relatively sharp limit visible to the eye where the montmorillonite seems to change from clear liquid to something more gel-like. The measured concentration profile reveals that at this limit the clay concentration is approximately doubled. Judging from the picture taken four days before the concentration profile was measured (Figure 6-1, 37 days) one would expect that the jump would be greater.

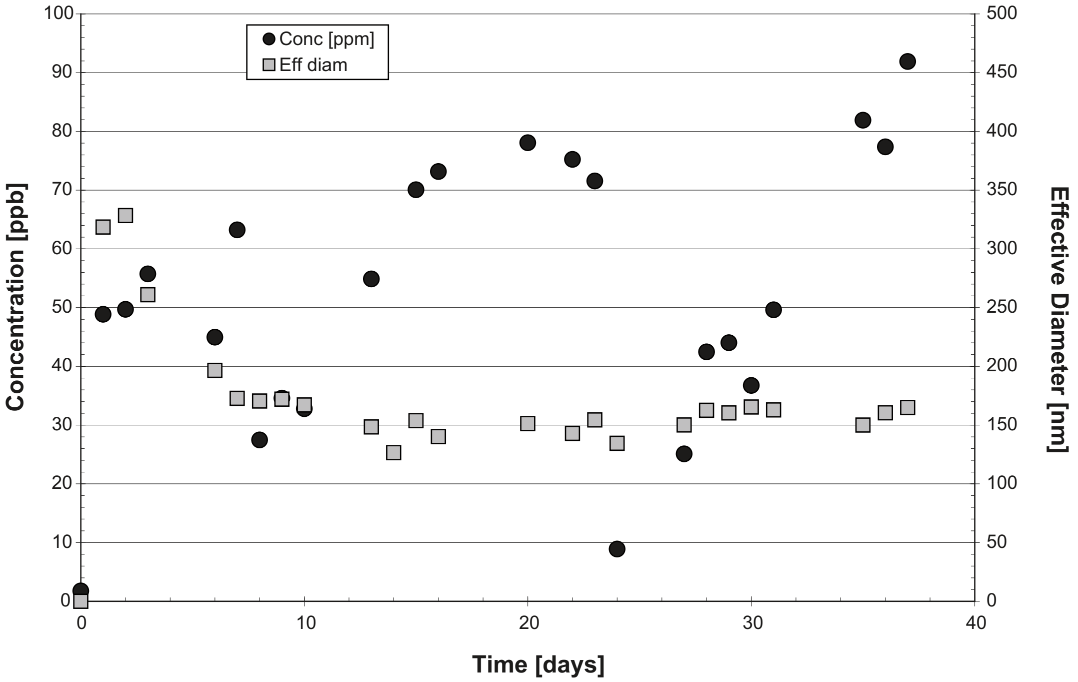

Figure 6-3. *Concentration and effective diameter of bentonite colloids as a function of time. After 7 and 23 days water was added to compensate the loss from the sampling.*

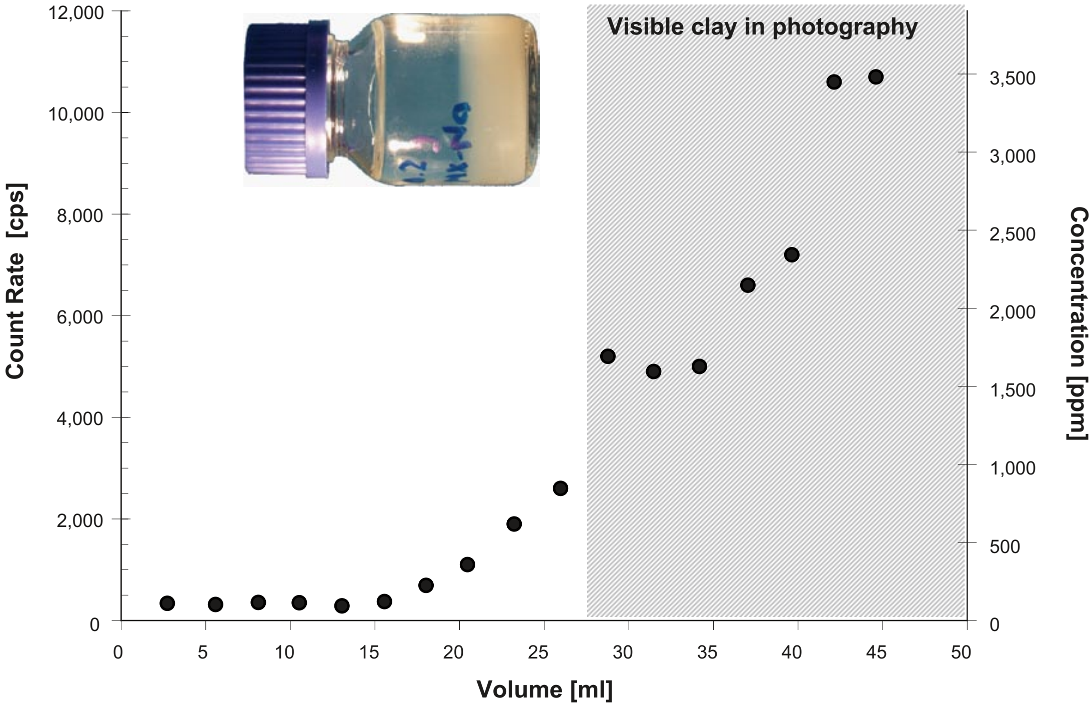

Figure 6-4. *Colloid concentration in each sample taken from the top of the bottle.*

7 Mineralogy of Dry Bentonite

When bentonite is manufactured it is ground to small grains which vary in size. In order to investigate whether it was possible to make the process of producing purified sodium montmorillonite more efficient, X-Ray Diffraction (XRD) studies were performed to see if the mineralogical composition varied with varying size.

Bentonite was sieved in size fractions >160, 160–140, 140–71, 71–45, 45–20 and <20 µm. The X-Ray diffraction patterns of the different size fractions together with un-sieved bentonite as reference can be seen in Figure 7-1. The intensity has been changed so that the different peaks from each sample can be identified.

The evaluation of the spectra (performed by Ola Karnland at Clay Technology, Lund) was made in detail for three of the samples (the reference bentonite, the fraction 160–140 µm and the smallest fraction <20 µm) and gave similar mineralogical composition as can be seen in Table 7-1.

The MX-80 Wyoming bentonite that was used in these studies thus seems to be relatively homogeneous and sieving the bentonite would not make the purification process any faster.

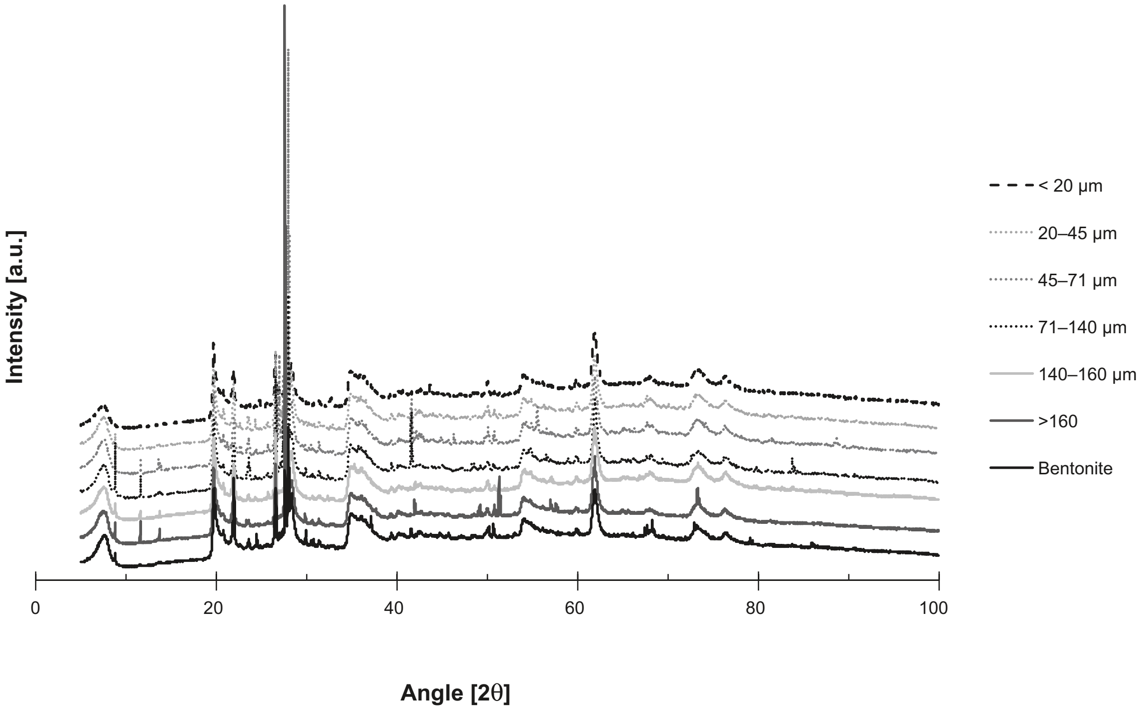

Figure 7-1. X-Ray Diffraction patterns of bentonite sieved to different sizes.

Table 7-1. Results from the XRD-study of the different size fractions.

Mineral	Bentonite	<20 µm	160–140 µm
Montmorillonite	76.0	77.1	72.4
Illite	2.6	3.2	1.8
Albite (high)	4.2	2.6	7.2
Albite(low)	0	0	1.9
Anorthite	0.8	0	0
Calcite	0	0.1	0.1
Cristobalite	4.6	3.7	3.1
Goethite	0.4	1.3	0.5
Gypsum	0.8	1	1.1
Hematite	0.7	0.5	0.5
Magnetite	0.8	0.6	1.2
Microcline (max)	0	0.1	0
Muscovite	0.8	0	1.5
Orthoclase	1.3	1.5	1.0
Pyrite	0.5	1.2	0.8
Quartz	4.3	4.6	4.5
Rutile	0	0.1	0.7
Tridymite	2.2	2.5	2.0

Errors are 1% in absolute values.

8 Artificial Fracture

8.1 Background

In the real situation compacted bentonite will be in contact with a water carrying fracture. The bentonite will swell out into the fracture due to the swelling pressure of the clay. Depending on the chemistry of the groundwater, the clay will continue to swell (disperse) into the fracture. This process is described in more detail by /Liu and Neretnieks 2006/.

In Japan an experiment called Bentflow /Matsumoto et al. 2008/ has been performed. The basic differences between Bentflow and the present experiment are:

- That in Bentflow the bentonite is introduced into the fracture as a plug in a hole drilled in the centre of the Plexiglas slab.
- Different bentonites were used.
- The water composition was different.
- Flow rates were different.

In Canada another similar experiment series have been carried out /Vilks et al. 2009/ where Plexiglas slabs also were used. Similarly to Bentflow a hole was drilled in the middle of the slabs and compacted bentonite was introduced as a plug in the hole. In the Canadian experiment the following parameters were varied in seven different tests:

- Distilled water and Grimsel water was used.
- The fracture aperture was either 1 or 5 mm.
- The bentonites used were MX-80, purified sodium and purified calcium montmorillonite.
- Flow rates.
- Inclination of the fracture (0 or 15 degrees).

8.2 Performance

To simulate a fracture a 50 × 50 cm Plexiglas slab was placed on top of another Plexiglas slab. The slabs were separated by 1 mm thick plastic cylinders. At one end of the slabs a 1 cm thick and 1 cm deep bentonite container was placed in direct contact with the fracture while the opposite end was blocked. Perpendicular to the bentonite container a distributor was located, which distributes water evenly over the whole side. Opposite to the distributor the flow is collected into 5 slots, see Figure 8-1 and Figure 8-2.

Bentonite compacted to a dry density of 1,000 kg/m^3 was placed in the bentonite container. The bentonite was then water saturated via a channel in the bottom of the container, Figure 8-3.

In the real case readily soluble accessory minerals in the bentonite (mainly gypsum) will dissolve and contribute to keeping the Ca^{2+}-concentration sufficiently high to prevent the montmorillonite from dispersing. Since the step where the accessory minerals dissolve were not the focus of these tests, the bentonite was pre-treated so that the readily soluble minerals would not play a role.

In the first fracture experiment bentonite with high montmorillonite content was used. The bentonite was prepared by first washing "regular" MX-80 bentonite twice (40 ml water/g clay) before it was centrifuged for 10 minutes in 6,000 rpm. The light part of the clay was collected. No attempts were made to cation exchange the clay and the Na^+/Ca^{2+} ratio was probably the same as that for MX-80 bentonite.

In the second fracture experiment bentonite that had been washed twice in order to remove readily soluble minerals (*i.e.* gypsum) was used. All other accessory minerals were thus present.

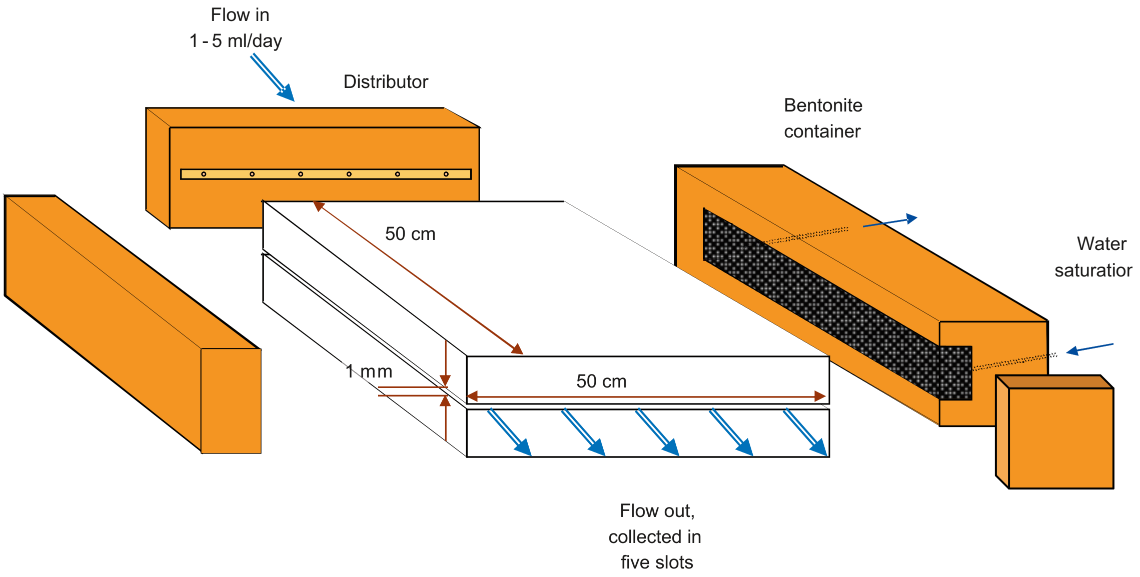

***Figure 8-1.** Principal drawing of the set-up for the experiments in the artificial fracture.*

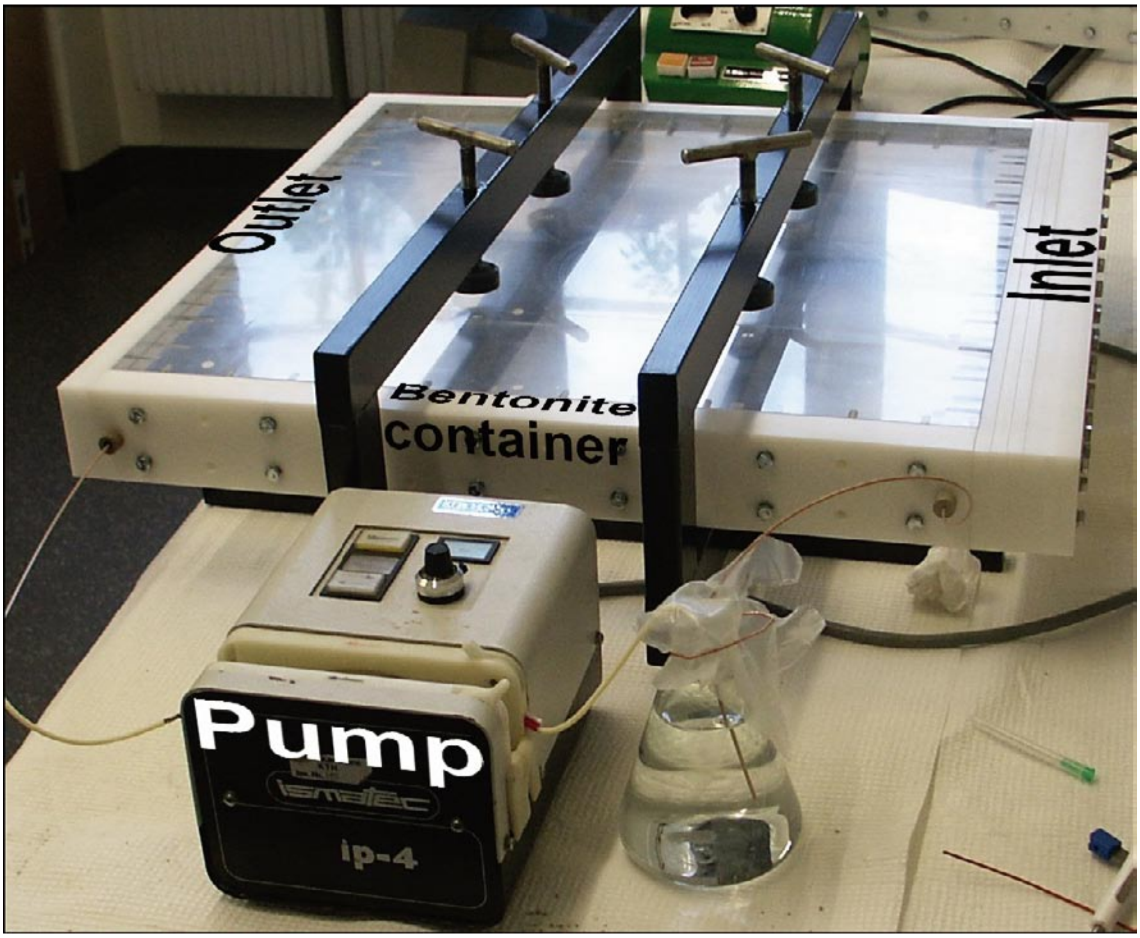

***Figure 8-2.** Artificial fracture. The bentonite is being water saturated.*

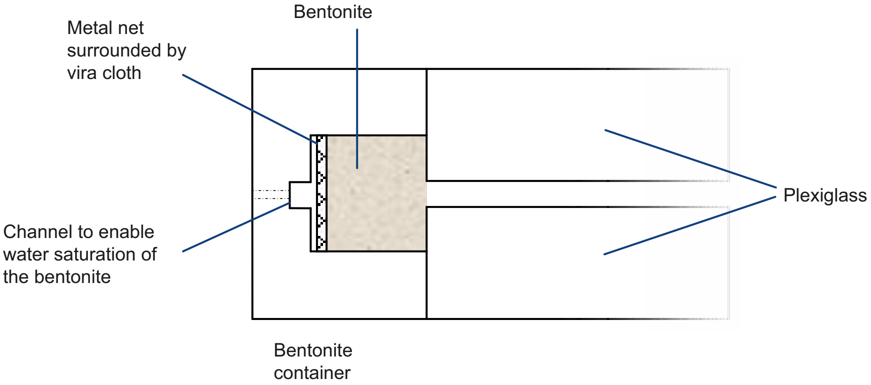

__Figure 8-3.__ Enlargement of the bentonite container.

8.3 Results and Discussion

The behaviour of the bentonite was more or less similar. After three weeks of water saturation the clay expanded into the fracture approximately 12–14 mm and did not expand further (Figure 8-4).

After three weeks the bentonite was fully water saturated (this based on scoping calculations and that no further expansion of clay into the fracture could be seen for a week of observation) and the channel at the bottom of the bentonite container was sealed. Distilled water was pumped with a low flow rate through the fracture. The clay started to disperse into the fracture more or less immediately, see Figure 8-5a, b and c.

As can be seen, clay disperse into the fracture. A clay concentration gradient can clearly be observed. Another interesting thing is the black rim that seems to be in the border where the bentonite seems to go from one state to another (gel to sol or whatever expression one prefers to use). The rim was observed in the first experiment (Figure 8-5c) but was even more pronounced in the second experiment (Figure 8-6) where the bentonite was only washed and not purified in any other way. When the experiment was terminated material from the rim was analyzed using XRD. Figure 8-7 displays a close-up photo of the rim.

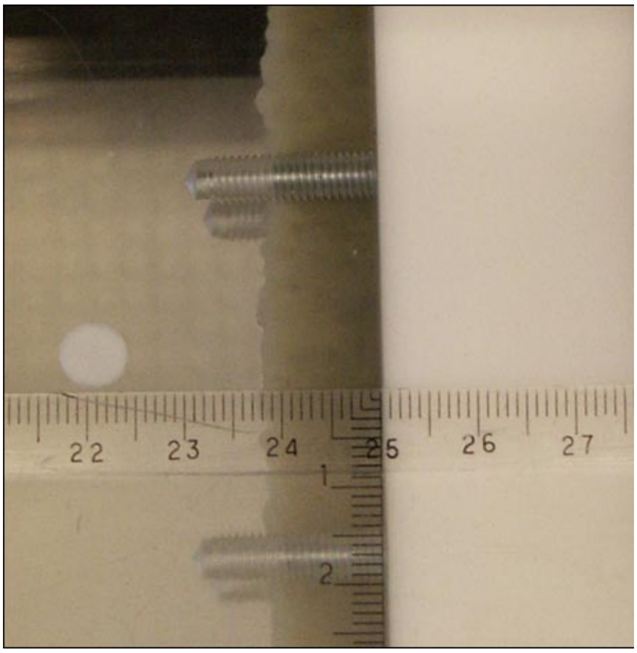

__Figure 8-4.__ After water saturation the bentonite had expanded 12–14 mm into the fracture.

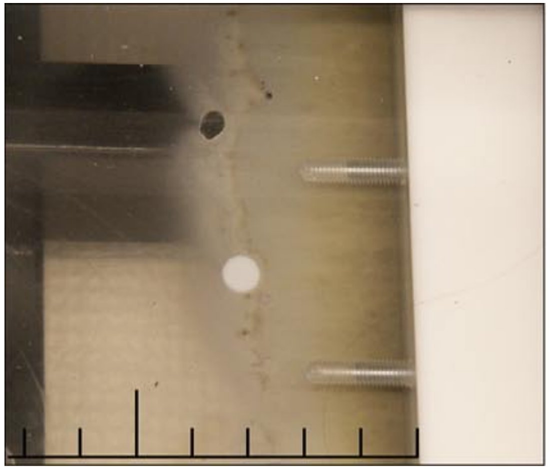

Figure 8-5a. After pumping distilled water in fracture water 4 weeks.

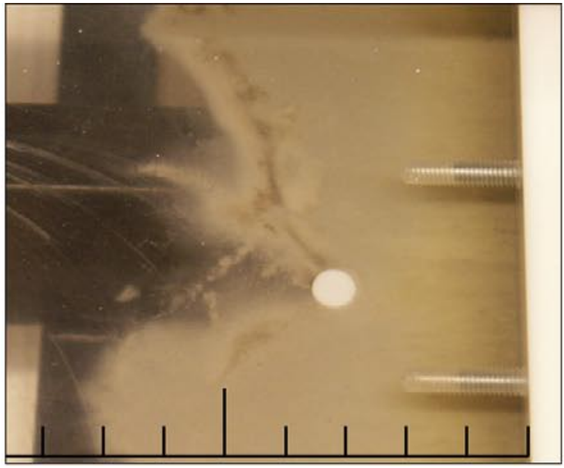

Figure 8-5b. After pumping distilled water in fracture water 28 weeks.

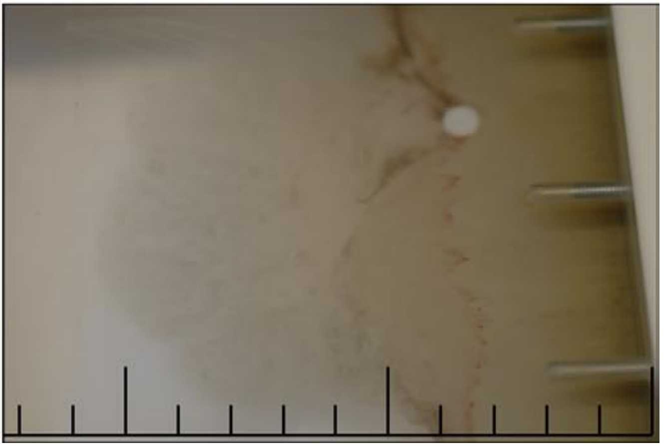

Figure 8-5c. After pumping distilled water in fracture water 45 weeks.

Figure 8-6. In the second experiment the fracture inclined a few degrees which caused the dispersed clay to sediment close to the inlet side.

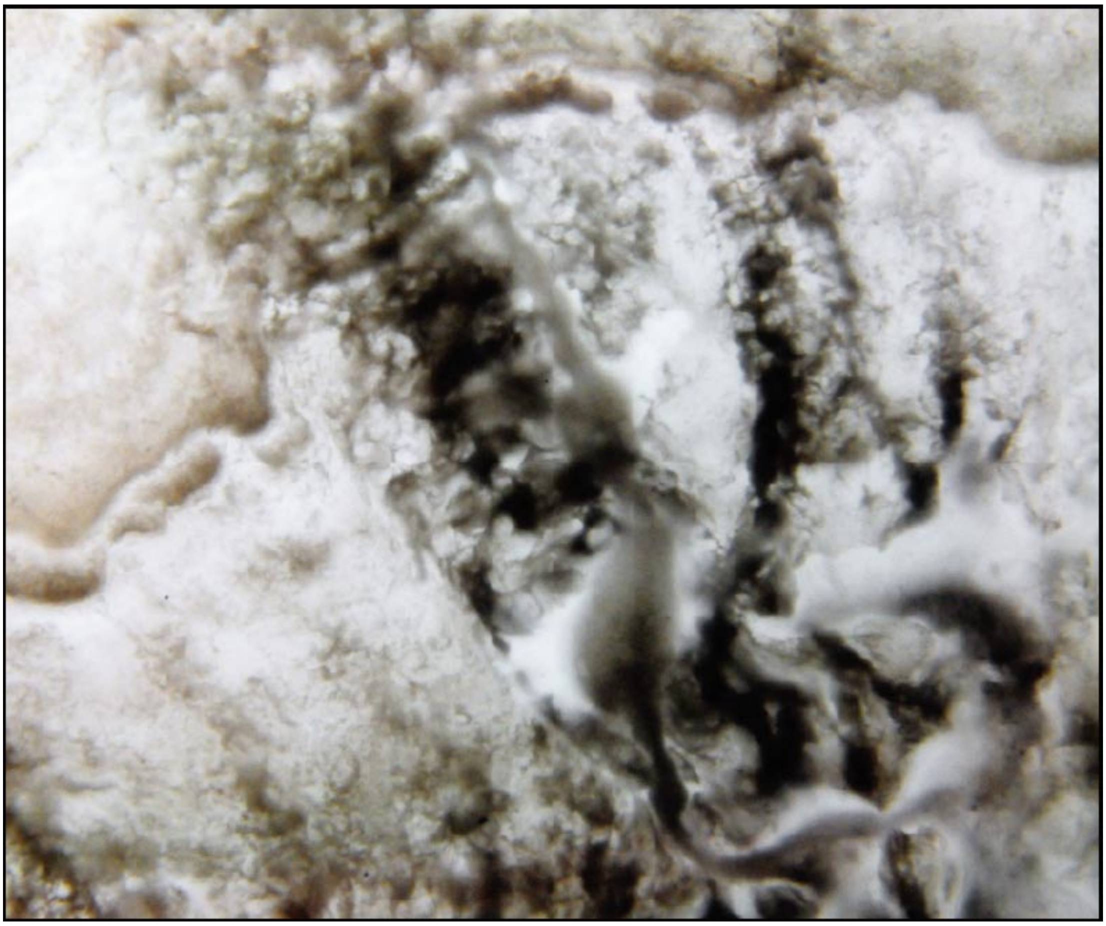

***Figure 8-7.** A dark rim was observed at the border where the clay seems to change phase from gel to sol.*

For comparison a MX-80 bentonite sample was analyzed as well as a sample taken from the bottom of the centrifugation tube when the bentonite was washed. When bentonite is dispersed in water and then centrifuged, one can clearly see two separate fractions, see Figure 8-8. At the top of the centrifugation tube is a light montmorillonite rich fraction and at the bottom is a darker fraction containing more accessory minerals. The darker fraction was collected, dried and analyzed as a reference in the XRD.

In Figure 8-9 and Table 8-1 the results from the XRD-measurements are displayed. As can be seen, the dark rim (as well as the centrifuged sample) contains a lot more feldspar (albite, anorthite, orthoclase and microcline) than the original MX-80 bentonite.

It was not possible to collect only material from the rim. Some of the material surrounding the rim was also collected. The montmorillonite content in the rim is probably much lower and one can most probably conclude that the rim consists of mainly feldspar but also some mica (muscovite) and quartz and resembles much the heavier fraction obtained when centrifuging bentonite.

In the second fracture experiment the fracture contained air bubbles that were hard to get rid of. Hence the fracture was tilted so that it inclined some 2–3 degrees (in the first experiment the fracture was also slightly tilted, about 1 degree). The higher end was at the water outlet. Surprisingly a relatively thick gel accumulated at the inlet of the fracture, i.e. not following the flow but sediments at the lowest point of the fracture, see Figure 8-6.

The most probable process for this behaviour is that when bentonite colloids leave the gel they have just overcome the attractive forces. Any collision with a neighbouring colloid will form a heavier colloid that is not stable and sediments. If there would be no inclination, the heavy colloid would end up at the bottom of the fracture and possibly later release smaller colloids due to the diluted water. However, our heavy colloid follows gravity towards a zone where the colloid concentration is higher and further collisions will make the colloid even more unstable.

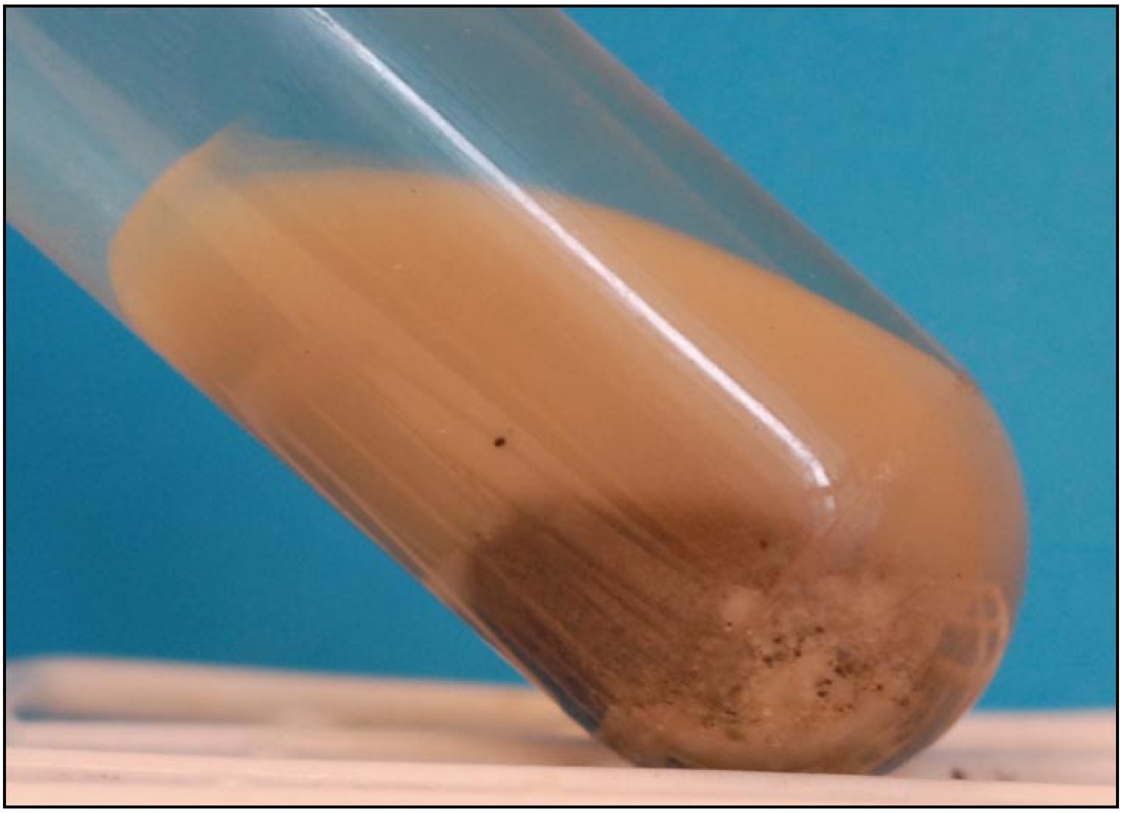

Figure 8-8. *MX-80 Bentonite that has been dispersed in water and then centrifuged. The lighter (both in colour and weight) fraction is montmorillonite rich, while the darker heavier fraction contains more accessory minerals.*

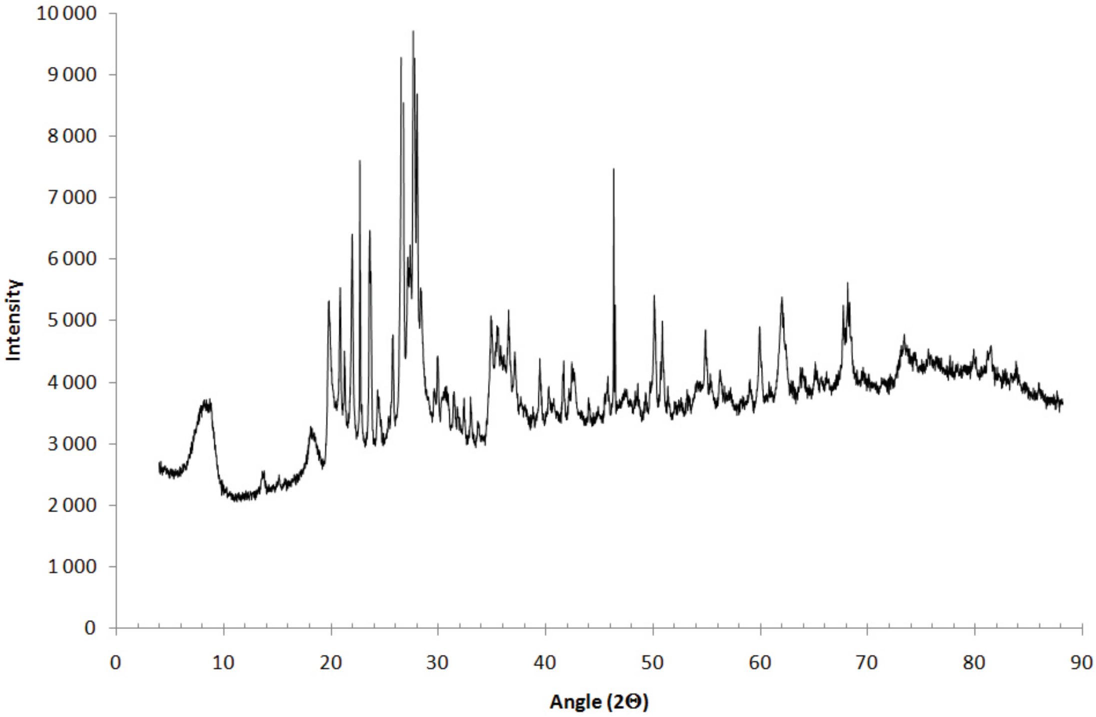

Figure 8-9. *XRD spectra of the dark rim that was found in the experiment with the artificial fracture.*

Table 8-1. Results from mineralogical XRD investigation of the rim, the bottom fraction when centrifuging MX-80 bentonite and a MX-80 sample.

Phase	Rim	Centrifuged sample	Bentonite MX-80
Montmorillonite	45	60.4	76
Feldspar[1]	39.4	25.8	6.3
Quartz	6.5	7.1	4.3
Muscovite	3.9	2.2	< 1
Gypsum	1.1	0.6	< 1
Pyrite	1	1.2	< 1
Goethite	1	0	< 1
Rutile	1	1.2	–
Tridymite	< 1	< 1	2.2
Lepidocrocite	< 1	–	–
Cristobalite	–	–	4.6
Illite	–	–	2.6
Calcite	–	–	< 1
Magnetite	–	–	< 1
Hematite	–	–	< 1

[1] Feldspar minerals that were found in the study: Albite, Anorthite, Orthoclase and Microcline.

The water flow through the fracture was not even. One test was performed to see how the flow path looked like using a blue dye (indigo carmine). As can be seen in Figure 8-10 the flow path was not steady and not even. This could also be seen in the collected samples. The collected volume of the bottles differed with time. During some time intervals almost no water was collected in some of the bottles, while other time intervals the same outlet channel gave the most water.

The water exiting in the five slots was collected in bottles. Spot tests of the bottles were taken and analyzed using PCS in the first experiment and the SPC in the second. The results can be seen in Figure 8-11 and Figure 8-12. The analyzes revealed that the samples are relatively uniform, independent of time after the experiment start and from what slot (how far from the bentonite container side of the fracture) the sample was taken.

Unfortunately the SPC was not available when the first experiment was performed and the samples could not be analyzed when the SPC was available, since microorganisms had started growing in the samples.

However, samples from the second experiment were measured on the PCS in order to compare the correlation between the two methods. Since most of the samples were consumed in the SPC measurements, the PCS measurements were performed on samples that were taken from the same slot at times close to those measured by SPC. The values of the colloid concentration varied between 0.03 and 0.11.

The measurements on the two instruments gave similar colloid concentrations in the outlet solutions for the two different experiments, even though the bentonite had been pre-treated slightly differently. In the first experiment most of the heavier accessory minerals had been removed while in the second experiment only the readily soluble accessory minerals were removed. This is not surprising, since accessory minerals with low solubility will not influence the chemistry of the system in a larger extent.

As can be seen in Figure 8-12, smaller sized colloids (up to 50 nm) are present in the highest concentrations. Larger colloids >100 nm are present in very low concentrations. Some of the smaller particles can be attributed to particles from the ion ex-changer in the water purification unit, see further section 4.2. However, this is probably not the only reason.

When calibration standards are measured on the SPC, four calibration curves are obtained for each standard, one for each channel (*i.e.* size range). What is read on the y-axis is the colloid concentration corresponding to that of a calibration standard (with the size distribution of the standard). If the size distribution of a sample has the same size distribution as the calibration standard the four measured channels should give the same result. However, this is not observed in Figure 8-12. Smaller sized colloids manage to follow the water flow, while lower concentrations of larger (>100 nm) particles were found in the outlet.

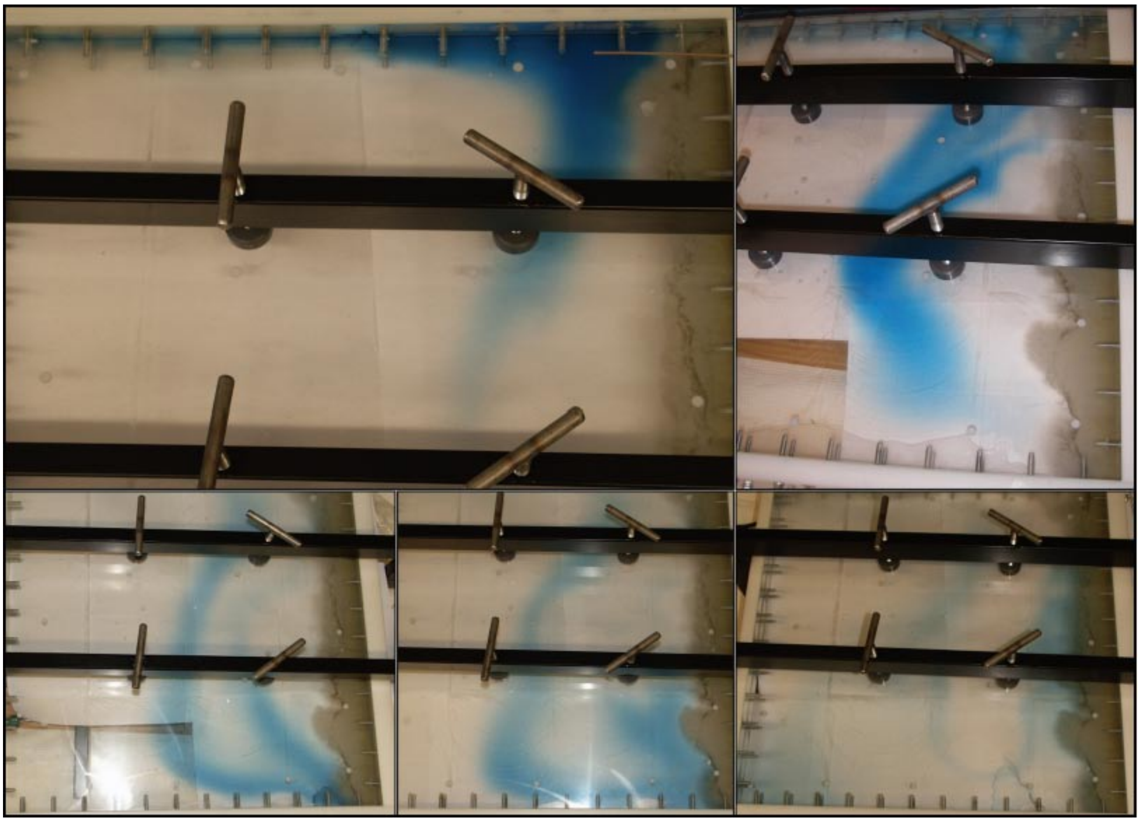

Figure 8-10. *To see how the flow path looked like a dye was added to the inlet solution. As can be seen the flow path varies a lot with time and is not evenly distributed.*

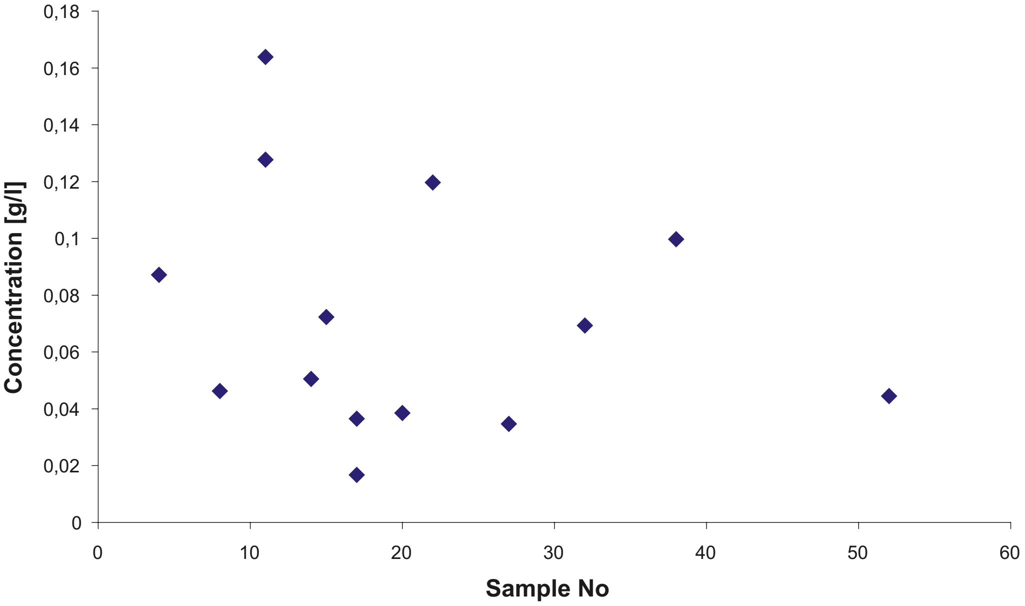

Figure 8-11. *Random samples from the outlet analyzed on the PCS from the first experiment in the artificial fracture. The sample number corresponds approximately to time with sample 50 being taken 45 weeks after water saturation. Points with the same sample number are taken at the same time from different outlet channels. No correlation could be seen between from what outlet-slot was taken.*

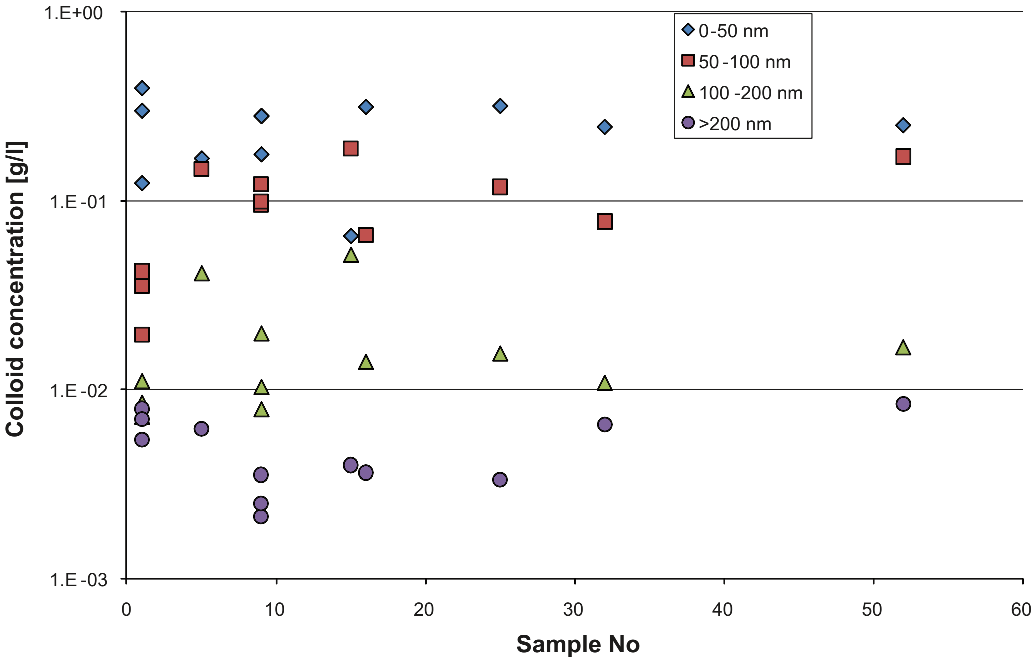

Figure 8-12*. Results from SPC analyses of randomly taken samples of the outlet solutions of the second experiment with an artificial fracture. The sample number corresponds approximately to time with sample 50 being taken 45 weeks after water saturation. Points with the same sample number and size fraction are taken at the same time from different outlet channels. Note that the concentrations are related to a calibration standard with a certain size distribution and not "true" values.*

Degueldre and various co-workers /Degueldre et al. 2009a, Bessho and Degueldre 2009, García-García et al. 2009/ have established that the concentration and size distribution of colloids that are formed in solution will be the same for solutions prepared from allowing bentonite to swell or from sedimentation of over saturated colloid suspensions. The size distribution in the calibration standards will, thus, be the same as that of the colloids which are released from the bentonite in the fracture. Hence, the observed difference in size distribution between the outlet solutions and the calibration standards are most probably due to the transport behaviour of the colloids. Smaller colloids follow the flow while larger colloids are affected by gravity in a greater extent.

To estimate the mass of the different fractions some assumptions have to be made. The first assumption is that the mass of a montmorillonite colloid is proportional to the square of the particle size (*i.e.* assuming the colloids have sheet-like structure). This assumption gives a greater potential mass loss of bentonite since the mass fraction of smaller particles (which was present in the highest relative amounts in the outlet) would have less impact assuming spherical geometry. If the mass is assumed to be proportional to the square of the particle size, the relative mass between the fractions can be calculated using equation 8.1.

The calculation for the fractions 0–50, 50–100, 100–200 and 200–300 nm gave a relative mass of 1:7:56:152, respectively (the size range 200–300 nm is also an assumption, since the channel measures particles larger than 200 nm). If the same calculation would be carried out assuming spherical geometry, which has been proposed by /Degueldre et al. 2009b/, the relative mass of the fractions would be 1:15:240:1040.

$$\text{mass interval in collids of } = \int_{size_1}^{size_2} s^2 \, ds \qquad \text{8-1}$$

The output signal of the SPC is directly proportional to the number of particles. It is thus possible to compare the number of particles found in each size range In Table 8-2 the average relative numbers of particles and their respective mass can be found.

One should, thus, be very careful when reading Figure 8-12. The two heaviest fractions make up more than 93% of the weight in the calibration standards and about half of the weight in the samples.

Table 8-2. Comparison of relative number of particles and mass in calibration standards and samples taken from the second experiment in the artificial fracture.

		Relative number of particles (average)		Relative mass of particles	
Size [nm]	Relative mass[a]	in calibration standards	in samples	calibration standards	samples
0–50	1	1	1	1	1
50–100	7	0.23	0.60	1.60	4.21
100–200	56	0.29	0.079	16.2	4.40
200–300[b]	152	0.12	0.0049	18.5	0.75
Sum				37.3	10.36

[a] Assuming that the mass of a montmorillonite colloid is proportional to the square of the size.

[b] The channel detects colloids larger than 200 nm. The range 200–300 nm is assumed in the calculations.

9 Conclusions

The test tube experiments showed that:

- Divalent cations (i.e. calcium) are the most important ions for keeping bentonite from dispersing. The critical calcium concentration obtained by this method was for sodium montmorillonite about 1–2 mM.
- The corresponding value for sodium is about 100 times greater.
- Untreated MX-80 bentonite does not disperse in this system.
- The CCC/CFC concentration of Ca^{2+} for MX-80 bentonite that had been washed twice (i.e. gypsum was removed) was found to be 2–3 mM using this method.
- The concentration of Ca^{2+} is the important parameter when determining CCC/CFC using this method, not the amount of available Ca^{2+} ions.

A concentration profile was obtained for swelling sodium montmorillonite.

XRD-studies showed that dry sieving MX-80 bentonite does not result in heterogeneities in mineral composition between the different size fractions.

The experiments in the artificial fracture between two Plexiglas slabs have showed that:

- Bentonite compacted to 1,000 kg/m^3 swells 12–14 mm into a fracture of the same surface roughness as that of Plexiglas and with an aperture of 1 mm.
- Montmorillonite rich clay and MX-80 that has been washed twice show similar dispersion behaviour in the fracture.
- A dark rim containing mainly feldspar was observed in the border where the bentonite seems to go from one state to another (gel to sol).
- Gravity plays a role in this system.
- The clay colloid concentration in the outlet of the fracture was less than 200 mg/l.
- The size of the colloids in the outlet of the fracture was much smaller than that obtained when MX-80 bentonite is dispersed in water.

10 References

Arcos D, Grandia F, Domènech C, 2006. Geochemical evolution of the near field of a KBS-3 repository, SKB TR-06-16, Svensk Kärnbränslehantering AB.

CRC Handbook of Chemistry and Physics 44th ed.

Degueldre C, Aeberhard P, Kunze P, Bessho K, 2009. Colloid generation/elimination dynamic processes: Toward a pseudo-equilibrium? Colloids and Surfaces A: Physicochem. Eng. Aspects 337, 117–126.

Degueldre C, Raabe J, Wold S, 2009. Investigations of clay colloid aggregates by scanning transmission X-ray microspectroscopy of suspensions, Applied Geochemistry 24, 2009, 2015–2018.

Bessho K, Degueldre C, 2009. Generation and sedimentation of colloidal bentonite particles in water, Applied Clay Science 43, 253–259.

Derjaguin B, Landau L, 1941. Theory of the stability of strongly charged lyophobic sols and of the adhesion of strongly charged particles in solutions of electrolytes, Acta Physico chemica URSS 14:633.

García-García S, Wold S, Jonsson M, 2007. Kinetic determination of critical coagulation concentrations for sodium- and calcium-montmorillonite colloids in NaCl and $CaCl_2$ aqueous solutions J. Colloid Interface Sci, 315(2), 512–519.

García-García S, Degueldre C, Wold S, Frick S, 2009. Determining pseudo-equilibrium of montmorillonite colloids in generation and sedimentation experiments as a function of ionic strength, cationic form, and elevation, Journal of Colloid and Interface Science 335, 54–61.

Goldberg S, Forster H S, Heick E L, 1991. Flocculation of Illite/Kaolinite and Illite/Montmorillonite Mixtures as Affected by Sodium Adsorption Ratio and pH. Clays and Clay Minerals, Vol. 39, No. 4, 375–380.

Karnland O, Olsson S, Nilsson U, 2006. Mineralogy and sealing properties of various bentonites and smectite-rich clay materials, SKB TR-06-30, Svensk Kärnbränslehantering AB.

Kryut H R, 1952. Colloid Sience, edited by Kruyt. Chapter VI, Overbeek J Th G, p 245. Elsevier Publishing Company.

Lagaly G, Ziesmer S, 2003. Colloid chemistry of clay minerals: the coagulation of montmorillonite dispersions, Advances in Colloid and Interface Science 100–102, 105–128.

Liu J, Neretnieks I, 2006. Physical and Chemical Stability of the Bentonite Buffer, SKB R-06-103, Svensk Kärnbränslehantering AB.

Matsumoto K, Iijima K, Kenji I, 2009. Erosion Phenomenon Evaluation of Bentonite Buffer Material Generation Behavior of Bentonite Colloid, JAEA Report, JAEA Research 2008-097.

Muurinen A, Lehikoinen J, 1997. Model for diffusion and porewater chemistry in compacted bentonite. Experimental arrangements and preliminary results of the porewater chemistry studies, POSIVA-97-02, Posiva Oy, Helsinki, Finland.

Neretnieks I, Liu J, Moreno L (In Preparation). Mechanisms and Models for Bentonite Erosion, Chapter 7: Pore water chemistry, Chemical Engineering and Technology, Royal Institute of Technology.

Plaschke M, Schäfer T, Bundschuh T, Ngo Manh T, Knopp R, Geckeis H, Kim JI, 2001. Size Characterization of Bentonite Colloids by Different Methods, Analytical Chemistry, 73(17) 4338–4347.

Puigdomenech, Ignasi, 2009. Chemical Equilibrium Diagrams. Computer code available at http:// w1.156.telia.com/~u15651596/ and www.kemi.kth.se/medusa.

Sposito Garrison, Holtzclaw, Kenneth M, Johnston, Cliff T, LeVesque-Madore, C S, 1981. Thermodynamics of sodium-copper exchange on Wyoming bentonite at 298°K., Soil Science Society of America Journal, 45(6), 1079-84.

Stumm W, Morgan JJ, 1996. Aquatic Chemistry 3rd Ed. Wiley & Sons Inc, NY.

Verwey EJW, Overbeek JThG, 1948. *Theory of the stability of lyophobic colloids*, Elsevier, Amsterdam.

Vilks P, Wold S, Miller N H, Vorauerc A, (In Preparation). *Bentonite erosion experiment in a synthetic fracture*.

Appendix I

The $CaCO_3$ solubility diagram is obtained from Medusa, which is part of Equilibrium Diagrams[1], a computer code written by Ignasi Puigdomenech. Medusa calculates various chemical equilibrium diagrams based on chemical equilibria, charge balances and stoichiometry. The following equilibria and constants are used by Medusa to calculate the $CaCO_3$ solubility diagram:

$CaCO_3(c) \rightleftharpoons CaCO_3$	$10^{-5.256}$
$H^+ + CaCO_3(c) \rightleftharpoons CaHCO_3^+$	$10^{2.955}$
$H^+ + CaCO_3(c) \rightleftharpoons CO_2(g) + CaOH^+$	$10^{-3.111}$
$CO_2(g) \rightleftharpoons H_2CO_3$	$10^{-1.468}$
$CO_2(g) \rightleftharpoons H^+ + HCO_3^-$	$10^{-7.82}$
$H_2O \rightleftharpoons H^+ + OH^-$	10^{-14}
$CaCO_3(c) + 2\ H^+ \rightleftharpoons CO_2 + Ca^{2+}$	$10^{9.669}$
$CO_2(g) \rightleftharpoons 2\ H^+ + CO_3^{2-}$	$10^{-18.149}$
$CaCO_3(c) \rightleftharpoons CO_2(g) + CaO(cr)$	$10^{-23.128}$
$CaCO_3(c) \rightleftharpoons CO_2(g) + Ca(OH)_2(c)$	$10^{-13.131}$

---

[1] www.kemi.kth.se/medusa

ISSN 1404-0344
CM Gruppen AB, Bromma, 2009